

Oil-Absorptive Polymeric Networks Based on Dispersed Oleophilized Nanolayers of Laponite Within Ethylene–Propylene–Diene Monomer Vulcanizates

H. A. Essawy,¹ M. M. Essa,¹ Z. Abdeen²

¹Department of Polymers and Pigments, National Research Center, Dokki 12311, Cairo, Egypt

²Petrochemicals Department, Egyptian Petroleum Research Institute, Nasr City 11727, Cairo, Egypt

Received 19 August 2008; accepted 29 January 2009

DOI 10.1002/app.30151

Published online 1 September 2009 in Wiley InterScience (www.interscience.wiley.com).

ABSTRACT: Oil-absorptive polymeric nanocomposites were prepared through the melt blending of soft oleophilic ethylene–propylene–diene monomer and stearyl acrylate as a hydrophobic monomer in the absence and presence of different loadings of untreated and oleophilized laponites with quaternary ammonium salts of *n*-alkylamines of different chain lengths (C10, C12, and C16) with dicumyl peroxide as a vulcanizing agent. The samples were then vulcanized at 152°C according to the determined rheometric characteristics to produce nanocomposite vulcanizates of an exfoliated type with limited cavities as revealed by

X-ray diffraction and scanning electron microscopy. The produced vulcanizates were evaluated as oil-absorptive polymeric networks and proved to be efficient oil sorbents of moderate activity. The oil absorptivity was examined with respect to the stearyl acrylate grafting, the types of oleophilizing agents of clay in comparison with the bare clay, and the clay loading and crosslink density. © 2009 Wiley Periodicals, Inc. *J Appl Polym Sci* 115: 385–392, 2010

Key words: blending; compatibility; composites; fillers; interfaces

INTRODUCTION

Several approaches have been introduced in the literature for the removal of aromatic compounds from water; among these approaches, gel-type polyurethane resins containing cyclodextrin units as specific sorption sites through the crosslinking of β -cyclodextrin with diisocyanates¹ and porous polymer sorbents containing amino groups and crosslinked with divinyl benzene (DVB) or ethylene glycol dimethacrylate² are suitable for the sorption of organic pollutants in water. Furthermore, both types of sorbents provide sorption capacities that are comparable to or higher than those of Amberlite sorbents (commercial resins).³ Because one of the most important criteria characterizing oil-absorptive polymers is a structural skeleton based on the formation of crosslinked, three-dimensional, hydrophobic networks that do not dissolve but swell in oil, it has been suggested that the interpenetrating polymer network technique could be a very useful method for the preparation of a crosslinked polymer.^{4,5}

In the work by Mei-Hua and coworkers,⁶ new crosslinked polymers and polymeric composites

comprising stearyl methacrylate, butyl styrene, and DVB were prepared, and they showed good physical strength and thus became candidates for use in the removal of spilt oil. The oil absorptivity decreased with increasing concentrations of DVB (which is necessary for improving the mechanical strength and accordingly the reusability of the resulting network) and *t*-butyl styrene.

Also, a series of oil gels based on the rigid hydrophobic monomer 4-*tert*-butylstyrene and the soft oleophile ethylene–propylene–diene monomer (EPDM) crosslinked with DVB were synthesized by suspension polymerization.⁷ It was stated that the equilibrium oil absorbency as well as the average molecular weight between crosslinks first increased and then decreased with an increase in the EPDM contents in the polymerization. Furthermore, an increase in DVB led to decreases in the equilibrium oil swelling and the molecular weight between crosslinks.

Atta and coworkers^{8,9} synthesized oil-absorptive networks based on 1-octene and isodecyl acrylate copolymers or pairs of 1-docosanylacrylate, cinnamoyloxy ethyl methacrylate, and methyl methacrylate in the presence of an initiator and 1,1,1-trimethylolpropane triacrylate as a crosslinker, and these proved to be highly efficient oil sorbents.

We believe that another approach based on a dispersed organoclay on a nanoscale within a polymer matrix via *in situ* intercalative polymerization^{10–13}

Correspondence to: H. A. Essawy (hishamessawy@yahoo.com).

can verify the purpose of strengthening the polymeric networks, which promotes oil retention under pressure and the repeated use of these matrices. Moreover, we hope that the anticipated uniform distribution of the organophilized nanoplatelets of the clay within the interpenetrating network matrix (increased aspect ratio) will cause a dramatic enhancement of the oil absorptivity. This article describes the aforementioned approach in detail and the impact thereof on the mechanical performance and oil absorptivity.

EXPERIMENTAL

Materials

N-Alkylamines (C10, C12, and C16) and stearyl acrylate (StA) were purchased from Aldrich Chemical Co. EPDM with 8% norbornene was a product of Bayer AG (Leverkusen, Germany). A commercial grade of dicumyl peroxide (DCP) was employed as a curing agent. Acetic acid was obtained from Sigma-Aldrich (Steinheim, Germany). Laponite RDS was provided by Southern Clay Products (Gonzales, TX). Crude oil was supplied from the El-Zaafrana oil field (Eastern Desert, Egypt).

Methods

Synthesis of the cationic surfactants

Different primary amines of various chain lengths (C10, C12, and C16) were dissolved in ethanol followed by stoichiometric amounts of acetic acid. The homogeneous mixtures were refluxed separately for 30 min. The ethanol was evaporated to finally obtain cationic surface-active agents in the form of pastes.

Laponite treatment

Laponite was converted to the oleophilized forms by the dispersion of calculated amounts of the corresponding surfactants according to the cation-exchange capacity (73 mequiv/100 g) into the lowest amounts of a water/ethanol mixture (70 : 30). Then, the clay was dispersed into the medium by stepwise addition under stirring within 5 min to prevent the formation of tactoids. The stirring was continued for another 2 h at 80°C. Afterwards, the clay was filtered and washed repeatedly with a water-ethanol mixture and finally was dried under reduced pressure for 3 days at 60°C.

Preparation of the EPDM rubber vulcanizates

The rubber (EPDM) was mixed with the various additives, StA, and organoclay on a two-roll mill

with an outside diameter of 470 mm at room temperature. The curing agent (peroxide) was then loaded after complete mixing, and the process was continued for another 5 min to induce graft polymerization/blending of StA to the norbornene terminus of EPDM. Finally, the curing characteristics of different EPDM mixes were derived from measurements on a Monsanto (USA) model 100 oscillating disc rheometer. The samples were cured at 152°C in an electrically heated hydraulic press for specific time intervals that ensured 90% curing according to the curing characteristics obtained with the rheometer. The vulcanized sheets (2-mm average thickness) were cut into dumbbell-shaped specimens (five replicates from each sample) for the evaluation of the physicomechanical properties.

Evaluation of the oil absorption

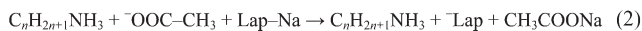
The oil absorption of the untreated laponite as well as the different oleophilized forms was evaluated with a spatula rub out test (ASTM D 281-95) using raw linseed oil. Briefly, 1 g of the clay powder was titrated with the lowest amount of oil that produced a very stiff, putty-like paste which did not break or separate. On the other hand, the dried polymers were cut into $1 \times 1 \text{ cm}^2$ pieces and immersed in toluene or diluted crude oil with toluene (10%) for 24 h and then taken out and tapped with filter paper to remove the excess oil from the surface. The weight difference divided by the weight of the dried polymer network gave the percentage of oil absorption (ASTM F 726-81).

Characterization

A Jasco (Tokyo, Japan) Fourier transform infrared (FTIR) 430 spectrometer was used for recording the IR spectra of the samples. The microstructures of the samples were examined in powder form (sheets in the case of rubber vulcanizates) with a Shimadzu (Kyoto, Japan) X-ray diffractometer with a Cu $K\alpha$ radiation source energized at 40 kV. The surface of the nanocomposites was examined with a JEOL (Tokyo, Japan) JXA-840A scanning electron microscope with a 30-kV operating voltage. The physicomechanical properties of the samples were evaluated with a Zwick (Ulm, Germany) 1425 tensile testing machine.

RESULTS AND DISCUSSION

Alkylamines of various lengths (C10, C12, and C16) were cationized by the addition of equimolar ratios of acetic acid to produce the corresponding alkyl quaternary ammonium acetates, which acted as cationic surface-active agents [eq. (1), Scheme 1].



Scheme 1 Synthesis of alkyl ammonium acetates and organophilization of laponite.

The produced cationic surfactants were subsequently used to replace the labile inorganic cations (Na^+ or Li^+) present between the layers of the laponite (six octahedral magnesium ions sandwiched between two layers of four tetrahedral silicon atoms) to convert the clay to the organoform in addition to a byproduct, CH_3COONa , which was washed out [eq. (2), Scheme 1].

The different laponite forms were elucidated with FTIR as shown in Figure 1; it is clear that in addition to the characteristic peaks of bare laponite [Fig. 1(a); 3637 and 3455 (OH stretching), 1047 ($Si-O$ stretching), and 400–600 cm^{-1} ($Si-O$ bending)], extra peaks evolved at 2858 and 2931 cm^{-1} , representing the aliphatic $C-H$ stretching of CH_2 and CH_3 groups of the surfactants [Fig. 1(b–d)].

As the laponite layers are held together by exchangeable cations (Na^+ or Li^+) that compensate for the negative charges which develop within the intergallery space because of a partial replacement of the magnesium of the octahedral layer with lithium, the treatment step is expected to increase the basal space of the clay as a result of the ammonium

salts extending their long alkyl chains within the basal space and occupying more room than the replaced Na^+ or Li^+ cations, which are smaller. This was confirmed by X-ray diffraction (XRD), which showed that the characteristic reflections of the clay ordered layers shifted to lower angles, giving rise to an expansion of laponite from 1.274 [Fig. 2(a)] to 1.4 [$C10-NH_3^+$ and $C12-NH_3^+$; Fig. 2(b,c)] and 1.6 nm [$C16-NH_3^+$; Fig. 2(d)]. Therefore, this organophilization is of great interest as the expanded basal space, which lies on the nanoscale, can be exploited as a nanoreactor for many chemical processes such as polymerization reactions and also as a base for tailoring oil-absorptive crosslinked polymers.^{4,5}

Besides, the presence of the long hydrocarbon chains fastened to the dispersed clay platelets should enhance significantly the oil/monomer absorption because of their hydrophobic nature and, in the mean time, the increased aspect ratio of the clay after the treatment. This postulation was confirmed by the measurement of the linseed oil absorption of the clay before and after the treatment with the cationic surface-active agents. The oil absorptivity of the clay (34 g/100 g) was nearly doubled for the treated clay with $C10-NH_3^+$ (71 g/100 g), tripled after the treatment with $C12-NH_3^+$ (102 g/100 g), and further enlarged to 121 g/100 g after the treatment with $C16-NH_3^+$. Interestingly, the XRD profiles shown in Figure 3 were in conformity with these data as the basal space of untreated laponite enlarged to 1.4 nm, whereas for the treated laponite, the hydrophobic-

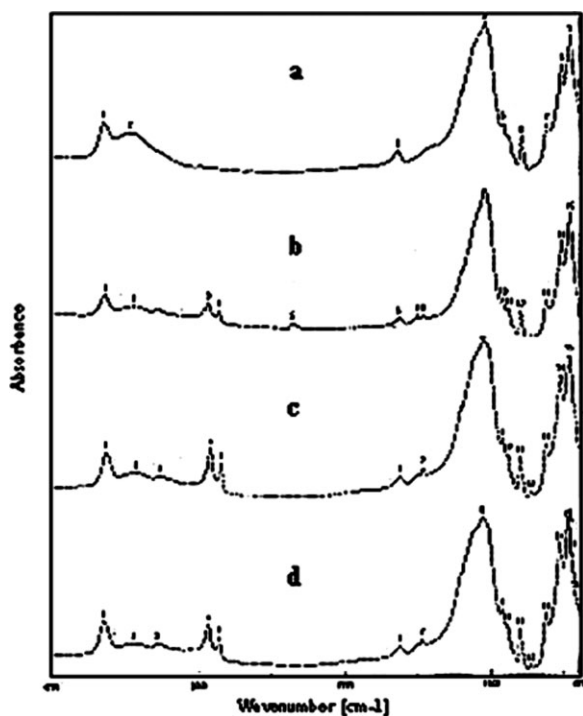


Figure 1 FTIR spectra of (a) laponite, (b) laponite- $C10$, (c) laponite- $C12$, and (d) laponite- $C16$.

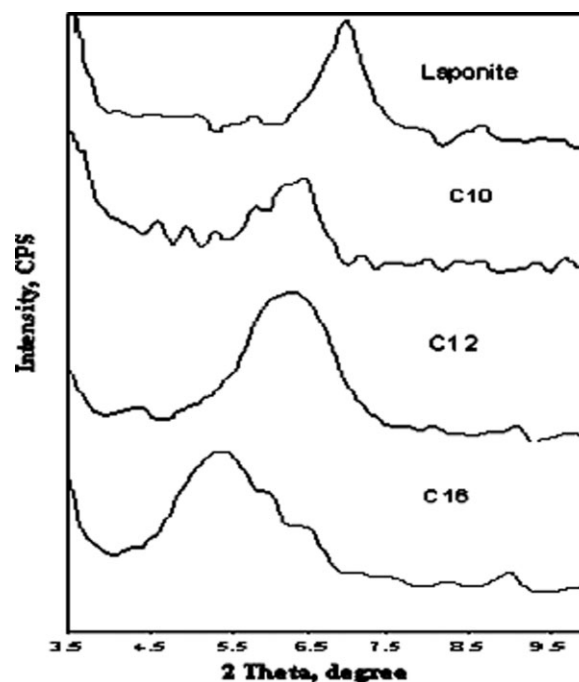


Figure 2 XRD profiles of (a) laponite, (b) $C10-NH_3^+$ -Lap, (c) $C12-NH_3^+$ -Lap, and (d) $C16-NH_3^+$ -Lap.

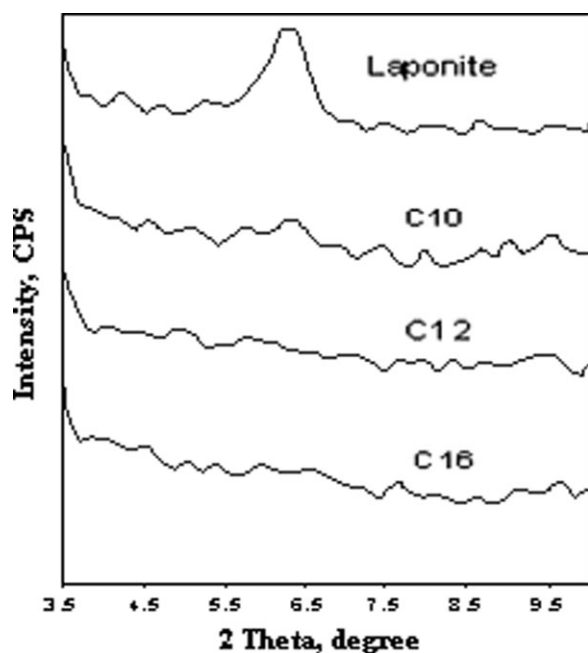


Figure 3 XRD profiles of (a) laponite, (b) C10-NH₃⁺-Lap, (c) C12-NH₃⁺-Lap, and (d) C16-NH₃⁺-Lap after the absorption of linseed oil.

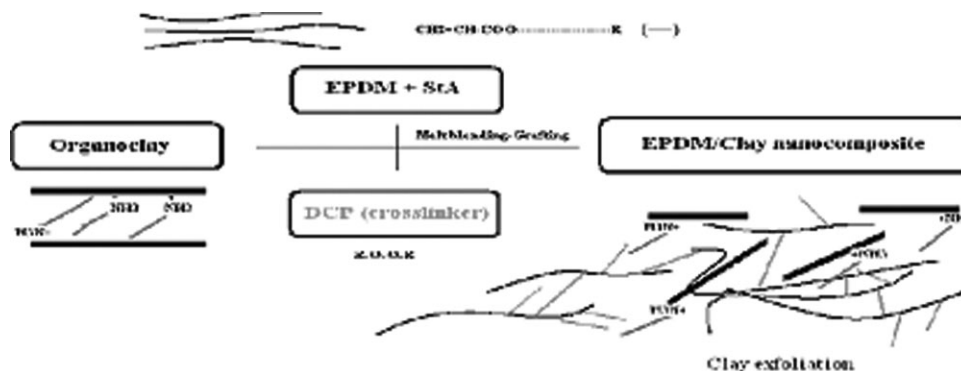
hydrophobic interactions between the anchored long alkyl tails within the basal space and the oil caused further expansion to the extent of exfoliation, which was indicated by the absence of any reflection pertaining to layer ordering.

Mei-Hua et al.⁶ reported that among the broad varieties of oil-absorptive crosslinked polymeric structures, crosslinked poly(stearylmethacrylate-*co*-divinyl benzene) had considerable tackiness, and its gels formed by oil absorption were ruptured because of their weak toughness, whereas crosslinked poly(4-*tert*-butylstyrene-*co*-divinyl benzene) had high brittleness and low oil absorptivity at an early stage despite its good strength after oil absorption. Conversely, the interpenetrating polymeric networks

did not have tackiness like crosslinked poly(stearylmethacrylate-*co*-divinyl benzene) or brittleness like crosslinked poly(4-*tert*-butylstyrene-*co*-divinyl benzene) but instead had good toughness after oil absorption.

Our suggested approach for further improving the mechanical performance of oil-absorptive nanocomposites is illustrated in Scheme 2. It is well known that a clay platelet after hydrophobization and dispersion within a polymeric matrix ensures a plasticizing effect in addition to a reinforcing action.^{14,15} Thus, the dispersion of the clay in its organophilic form within a hydrophobic matrix such as EPDM, in the presence of an oleophilic comonomer (StA) and a crosslinker (DCP), is liable to be further intercalated with higher proportions of all these components concurrently by melt blending because of the hydrophobic-hydrophobic interaction. As a result, the grafting polymerization of StA onto EPDM can take place during the melt blending at an elevated temperature caused by friction. The postcuring process can be completed at a higher temperature in the presence of the crosslinker (DCP) according to the rheometric characteristics, and this leads lastly to the formation of a polymeric network. It is expected that these conditions will contribute to the intercalation/exfoliation of the clay according to a previous study, which reported the intercalation of an organoclay into EPDM grafted with maleic anhydride or glycidyl methacrylate as a compatibilizer with sulfur as a curing agent: the processing conditions were found to contribute strongly to the clay intercalation/exfoliation.¹⁶ This should be the main cause of any augmentation/diminishment in the oil absorption.

It is well recognized that chemical crosslinking with peroxide has the function of strengthening EPDM as it increases the number of crosslinks and hence the interactions among the chain segments if high concentrations are used. However, excessive crosslinking could lead to stress concentration, which reduces the network strength.⁷ This problem



Scheme 2 Preparation of an oil-absorptive nanocomposite based on oleophilized laponite.

TABLE I
Rheometric Characteristics, Oil Absorptivity, and Mechanical Properties of Different EPDM Vulcanizates as a Function of the Contents of Clays of Different Natures in the Presence of StA

	Sample									
	M1	M2	M3	M4	M5	M6	M7	M8	M9	M10
Formulation										
EPDM	100	100	100	100	100	100	100	100	100	100
StA	—	6	6	6	6	6	6	6	6	6
Laponite	—	—	4	8	—	—	—	—	—	—
C10-NH ₃ ⁺ -Lap	—	—	—	—	4	8	—	—	—	—
C12-NH ₃ ⁺ -Lap	—	—	—	—	—	—	4	8	—	—
C16-NH ₃ ⁺ -Lap	—	—	—	—	—	—	—	—	4	8
DCP	1.5	1.5	1.5	1.5	1.5	1.5	1.5	1.5	1.5	1.5
Rheometric characteristics										
M_H (dNm)	78	80	78	71	80	70	78	81	54	68
M_L (dNm)	19	16	16.5	16	13.5	15.5	15	17	20	16
ΔM (dNm)	59	64	61.5	55	66.5	54.5	63	64	34	52
Time for attaining 90% cure (min)	22	21.25	21.75	20	20.25	20.25	20	20.25	20	20
Scorch time (min)	2.25	2	1.75	1.75	1.75	1.5	1.5	1.75	1.5	1.5
Cure rate index (min ⁻¹)	5.1	5.2	5	5.47	5.4	5.33	5.4	5.4	5.4	5.4
Physicomechanical properties										
Tensile strength (MPa)	0.86	0.84	1.2	1.21	0.99	1.235	1.252	1.44	1.244	1.1
Elongation at break (%)	195	236	297.4	373	254	287.4	335	292	315	314
Swelling in toluene (%)	219.3	235.5	247.4	274.1	231.6	236.5	235.4	236.7	253	260
Swelling in crude oil (%)	216.5	232.4	243	270	228.4	228	233.1	238.2	248.1	253.5
Soluble fraction (%)	0.86	4.52	4.3	4.04	4.59	4.64	4.56	4.15	4.21	4.3

may be overcome by the incorporation of a plasticizing modifier that weakens the chemical crosslinking strength by forming a relaxed network structure,¹⁷ which should have a positive influence on the oil absorbency. StA as a modifier can be introduced as grafted side chains through the norbornene termini during the melt blending process to play this role by increasing the free space between chains, which will become accessible for oil absorption. The same role can be played synergistically by the organoclay as a reinforcing material that at the same time has a plasticizing effect and should further act in favor of oil absorbency.

Table I lists the tunable parameters of this reaction, which are the clay content, the length of the hydrocarbon chain of the treating alkyl ammonium acetate, and the curing conditions, determined according to the derived rheometric characteristic data.

Table I reveals that the time for attaining 90% cure, the curing onset or scorch time, and the cure rate index changed slightly with the variation of the clay loading in either its modified form or neat form in comparison with the blank sample (M1), which contained neither clay nor StA, or the sample with StA in the absence of any clay (M2). On the other hand, the impact of the compounding was generally more prominent on both the minimum torque (M_L) and maximum torque (M_H). M_L decreased slightly with more clay loading of the untreated form (M3 and M4) but increased with more loading upon treatment with C10-based laponites (M5 and M6) and C12-based laponites (M7 and M8) and then

decreased with the chain length of the intercalating agent increasing to C16 (M9 and M10). On the other hand, M_H was also affected, particularly for the loaded samples with C16-treated laponite; it increased with more loading of laponite (M9 and M10). This can be attributed to the fact that the reinforcing action of the laponite is balanced by the plasticizing action of the treating agents of the clay on the one hand and by the lubricity of the grafted chains of StA on the other hand. Moreover, even the laponite itself in its untreated form can act as a plasticizer, especially once defoliated.

Table I also lists the alterations in the mechanical properties of the EPDM nanocomposite vulcanizates in terms of the tensile strength and elongation at break, revealing significant changes as functions of the grafting of StA, the clay loading, and the type of intercalant; this holds mainly for different network characteristics according to all the listed parameters. As far as the insertion of grafted StA chains is concerned, the elongation at break was enhanced, whereas the tensile strength remained constant, and this proves the assumption (cf. M1 and M2).

M3 and M4 revealed that the untreated laponite could play a dual function as a stiffening agent and a plasticizer at the same time, so both the tensile strength and elongation at break increased in comparison with M1 and M2. This parallel enhancement can most likely account for a uniform distribution of exfoliated platelets of laponite within the EPDM matrix during the melt blending,¹⁶ even without any preintercalation, as the whole system contained ester

sites that belonged to the acrylate groups, which potentially contributed to the exfoliation of the laponite platelets; such an effect is expected to be further enhanced in the presence of grafted StA chains. The expected lubricative effect that may be imposed by the intercalating agents with their long hydrocarbon tails could not be investigated for the rest of the formulations (M5 and M6, M7 and M8, and M9 and M10) as they followed the same trend.

This situation may in fact be realized by the prevalence of exfoliated clay platelets as plasticizing agents; their effect is further assisted by the presence of grafted StA chains. All these factors work in a combinatorial fashion and permit us to modulate both the tensile strength and elongation at break. Therefore, the impact of the aforementioned factors on the mechanical integrity of the samples may be correlated with the oil absorptivity (swelling in toluene and crude oil).

The blank (M1) absorbed 219% of the toluene on a weight basis, and this increased slightly to 235% upon the grafting of StA (6 phr) in the absence of any form of laponite (M2). A further elevation in the toluene absorbency was noticed with the simultaneous loading of untreated laponite (247% for M3 with 4 phr and 274% for M4 with 8 phr), whereas this ratio collapsed upon the pretreatment of laponite with C10 (M5 and M6) and C12 (M7 and M8) as intercalating agents, regardless of the loading of treated laponite, which seems to play no role in this respect. However, the absorbency of toluene started to re-increase after the pretreatment of laponite with an intercalating agent bearing a longer chain with 16 carbon atoms (M9 and M10), but it did not reach the absorbency level of M4 (274%, the maximum toluene absorbency of all formulations). These absorbencies are inferior with respect to those obtained by other researchers^{6,7} with consideration of the difference in the nature of the crosslinked structures and the absence of particulate fillers. Also, it should be kept in mind that the defoliation of clay platelets, especially after the pretreatment and subsequent uniform distribution, leads to intensive hydrophobic–hydrophobic interactions resulting in occupation of the cavities or other free spaces between the chains. Therefore, weak oil absorption may be obtained, and the same can happen when filler particulates reagglomerate; this leads to a collapse in the basal space (M6; Fig. 4), whereas for the untreated laponite, elevated polar–polar interactions with the ester groups of the StA may lead to strengthening.

The aforementioned data can be supported on the one hand by XRD (Fig. 4), which reveals that the samples exhibited approximately fully exfoliated microstructures for all formulations, even for M4, whereas surprisingly the laponite of M6 collapsed and acquired almost a basal space that was the same

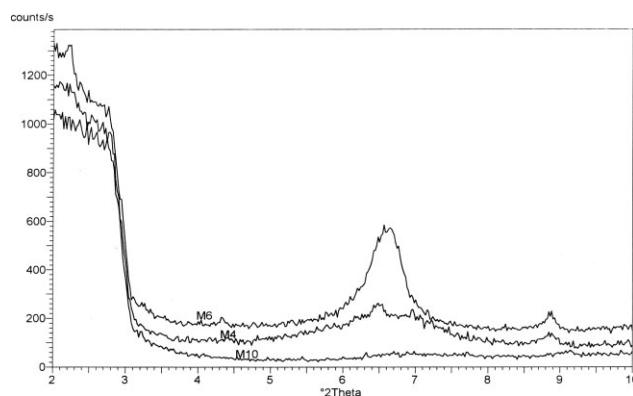


Figure 4 XRD profiles of EPDM nanocomposite formulations: (a) M4, (b) M6, and (c) M10.

as or even narrower than that of its corresponding treated laponite. This additional interlayer decrease was reported as a phenomenon most likely to occur during the processing of nanocomposites based on thermoset rubbers,¹⁶ such as natural rubber and epoxidized natural rubber, and this suggests that the amine modifier has been removed, at least in a given portion of the clay. Even though the characteristic peak referring to M6 is nearly the same as that of its corresponding treated laponite, it is broad and of trivial intensity, so it may also be handled as belonging to a remaining portion of clay not involved in the subsequent intercalation process during vulcanization. Scanning electron microscopy (SEM) showed, on the other hand, that M2 was characterized by the presence of free volume, mostly hidden by a surface-migrated unpolymerized StA [Fig. 5(a)], which is thought to have developed as a result of the grafting process.

After the incorporation of the untreated laponite (M3 and M4), the grafting changed the surface topography, and no migration of unreacted StA could be detected; also, the laponite in its untreated form could not be recognized [M4; Fig. 5(b)] to any further extent. This may emphasize its coverage with the grafted chains through polar–polar interactions of the ester groups, and this agrees absolutely with the XRD. Moreover, the free volume within the produced nanocomposites was not affected by the incorporation of laponite in its untreated form.

The unexpected drop in oil absorptivity after the treatment of laponite with the C10-based modifier (M5 and M6) may be indicated by the system turning to elevated hydrophobic–hydrophobic interactions between the EPDM and grafted chains on the one hand and the oleophilized laponite platelets on the other hand, and this might be one of the reasons for the interlayer space of a base laponite in any formulation collapsing, especially at a critical loading (M6). However, this was found to be for the sake of the grafting process as the grafted chains became

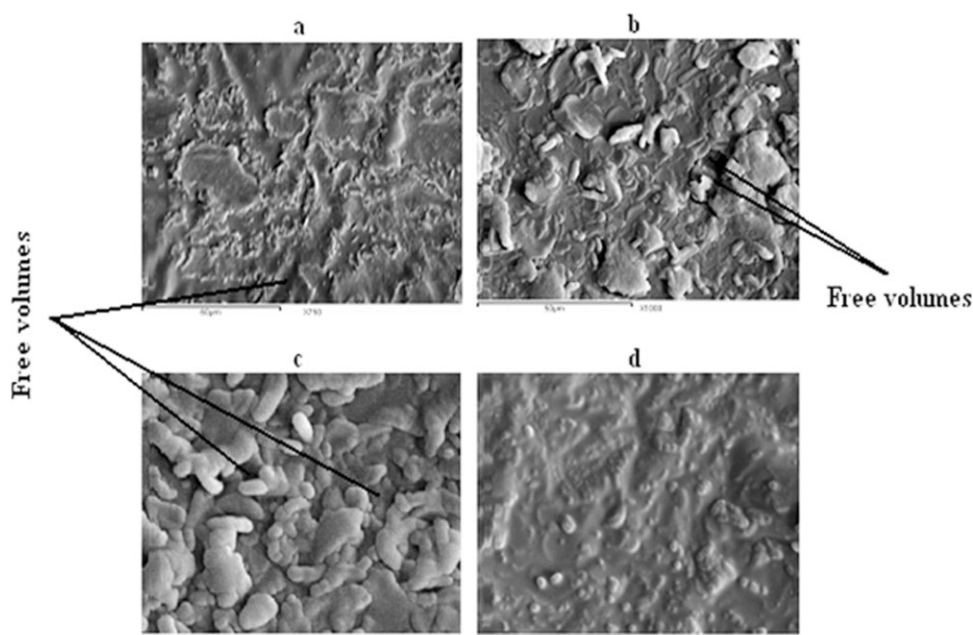


Figure 5 SEM images of (a) M2, (b) M4, (c) M6, and (d) M10.

entangled, more uniform, and denser on the surface; this seems to be the reason for the constricted free volume [M6; Fig. 5(c)], so these observations lie once more in accordance with the XRD.

There was a further rise in the oil absorptivity of the samples when the chain length of the intercalating agent (modifier) of laponite was increased to C12 (M7 and M8) and C16 (M9 and M10); this can be considered to some extent comparable to the cases in which untreated laponite was employed (M3 and M4). It may be surprising that this was associated with complete vanishing of any free space [M10; Fig. 5(d)], which can account for this rise unless the chain length of the modifier is considered to have induced more oil absorption via the intensified hydrophobic–hydrophobic interactions, even if the available free space became exclusively limited to accommodate the oil.

It is imperative to notice from the table that the soluble fraction, which was about 0.86% for M1 and intensified to approximately 4% for the rest of the formulations (M2–M10), may be ascribed to a small amount of unreacted EPDM or DCP or most likely a considerable portion of unreacted or homopolymerized StA that did not contribute to the formed network structure. It is worth mentioning that the toluene absorptivity should increase by 5–7% for all the samples (but decrease to 1% for M1) because of the weight loss due to soluble fractions. On the other hand, the crude oil absorbency was very similar to the case of swelling in toluene; it showed slightly lower values but followed the same trend. However, when the soluble fractions was taken into consideration, the ratio of oil absorbency increased by 6–7%

for all the samples, except for M1, for which it declined to 1.4%.

It was reported by Arroyo et al.¹⁸ that the difference between M_H and M_L ($\Delta M = M_H - M_L$) can be taken as a measure of the extent of the crosslink density in rubber phases. In view of that, some points can be drawn from Table I: the insertion of StA grafting (M2) stimulated higher crosslink density with respect to M1 in contrast to our expectations. Nevertheless, the oil absorptivity increased in toluene and crude oil. When the loading of untreated laponite was doubled, the crosslink density decreased, and this led to enhanced oil absorptivity in both toluene and crude oil (M3 and M4). Such behavior could not occur unless the laponite was exfoliated into individual platelets, and this further proves our assumption of the existence of some interaction between the polar surface of the platelets and the polar ester sites of the grafted acrylate chains.

Replacing the laponite with the treated one based on C10 did not provoke a significant alteration in the crosslink density. However, a small drop in swelling in both toluene and crude oil was noticed (M5 and M6). Very close data were obtained when the chain length of the intercalating agent was increased to 12 carbon atoms (M7 and M8). When we were dealing with M9 and M10, a continuous decline in the crosslink density was noticed. It seems that the intercalating agent (with 16 carbon atoms) exceeded a critical length of the hydrocarbon tail, thereby leading to a competition between the lubricating effect of the exfoliated nanoplatelets and their stiffening effect originating from the intensive

hydrophobic–hydrophobic interaction, which could be confirmed also by the higher swelling values in the case of untreated laponite; consequently, the situation became complicated as some of the aforementioned parameters work synergistically, whereas others work antagonistically.

CONCLUSIONS

EPDM nanocomposite vulcanizates with laponite as a nanodispersed phase, having different network characteristics (mainly the crosslink density), can be prepared by a graft/melt blending technique for applications as oil sorbents. Many variables, including the grafting of StA, intercalating agents of the clay, and clay loading, can be employed for further enhancing the oil-removal efficiency in the future.

References

1. Kitamura, M.; Mizobuchi, Y.; Tanaka, M.; Shono, T. *Bull Chem Soc Jpn* 1981, 54, 2487.
2. Martel, B.; Morcellet, M. *J Appl Polym Sci* 1994, 51, 443.
3. Jahangir, L. M.; Samuelson, O. *J Chromatogr* 1980, 193, 197.
4. Satoshi, M.; Shin-Ichi, K.; Zenjiro, O. *Polymer* 1993, 34, 2845.
5. Frisch, H. L.; Frisch, K. C.; Klemperer, D. *Pure Appl Chem* 1981, 53, 1557.
6. Mei-Hua, Z.; Seung-Hyun, K.; Jong-Gu, P.; Chang-Sik, H.; Won-Jei, C. *Polym Bull* 2000, 44, 17.
7. Wu, B.; Zhou, M.; Lu, D. *Iranian Polym J* 2006, 15, 989.
8. Atta, A. M.; Arndt, K. F. *J Appl Polym Sci* 2005, 97, 80.
9. Atta, A. M.; El-Ghazawy, R.; Farag, R. K.; El-Kafrawy, A. F.; Abdel Azim, A. A. *Polym Int* 2005, 54, 1088.
10. Essawy, H. A.; Badran, A. S.; Youssef, A. M.; Abd El-Hakim, A. A. *Macromol Chem Phys* 2004, 205, 2366.
11. Essawy, H. A.; Badran, A. S.; Youssef, A. M.; Abd El-Hakim, A. A. *Polym Bull* 2004, 53, 9.
12. Essawy, H. A.; Badran, A. S.; Youssef, A. M.; Abd El-Hakim, A. A. *Polym Plast Technol Eng* 2008, 47, 66.
13. Essawy, H. A. *Colloid Polym Sci* 2008, 286, 795.
14. Abd El-Hakim, A. A.; Badran, A. S.; Essawy, H. A. *Polym Plast Technol Eng* 2004, 43, 555.
15. Essawy, H. A.; Abdelwahab, N. A.; Abd El-Ghaffar, M. A. *Polym Degrad Stab* 2008, 93, 1472.
16. Gatos, K. G.; Thoman, R.; Karger-Kocsis, J. *Polym Int* 2004, 53, 1191.
17. Cai, J. J.; Salovey, R. *J Mater Sci* 2001, 36, 3947.
18. Arroyo, M.; Lopez-Monchado, M. A.; Herrero, B. *Polymer* 2003, 44, 2447.